Suppression of reverse flows in pumping by induced-charge electro-osmosis using asymmetrically stacked elliptical metal posts

Hideyuki Sugioka*

Frontier Research Headquarters, Canon Inc. 30-2, Shimomaruko 3-chome, Ohta-ku, Tokyo, Japan

(Received 23 June 2008; revised manuscript received 29 October 2008; published 25 November 2008)

Several researchers have analyzed pumps that employ induced-charge electro-osmosis (ICEO) using mainly coplanar electrode array structures in a lateral electric field. We propose ICEO pumps that remove reverse flows using asymmetrically stacked elliptical metal posts and numerically examine the pumping performance. By the boundary element method along with double layer approximation, we find that the asymmetrical stacking configuration efficiently suppresses the unwanted reverse flow and yields velocities of the order of a few millimeters per second, and this configuration is compatible with that of an optimized half-coating pump. Further, we propose a simple model for the stacking pump and predict that the velocity of such a stacking pump with a thin limit is larger than 67% of that of a circular cylindrical half-coating pump of the same length. Using this stacking pump, we can expect to significantly improve the pumping performance.

DOI: 10.1103/PhysRevE.78.057301 PACS number(s): 47.61.Fg, 47.57.jd, 82.47.Wx, 82.45.−h

In an ionic solution, metal is polarized and screened by surrounding ions. Since an applied field $\boldsymbol{E}$ acts on its own induced diffuse charge, the representative slip velocity U_b on the metal surface is proportional to $\boldsymbol{E}^2$. This nonlinear phenomenon is called induced-charge electro-osmosis (ICEO) [1,2]. Recently, pumps that employ ICEO with broken symmetry were proposed, and they have attracted considerable attention [3–7] because they have a large flow velocity ($\sim$mm/s) with a small voltage ($\sim$V) and can prevent the occurrence of dc problems such as chemical reactions in an electrolytic solution. These pumps are usually fabricated and analyzed by considering planar structures (structures made by a thin film process) because the fabrication of planar structures is easier than that of high-aspect-ratio structures (structures in which the ratio of the height to the width is high). However, by the development of process technologies such as deep reactive ion etching, the fabrication of high-aspect-ratio structures has also become a realistic option.

Bazant and Squires [1,2] proposed the following high-aspect-ratio pumps using asymmetrical ICEO flow around metal posts: (1) a half-coating metal pump, (2) an irregular-shaped metal pump, and (3) an asymmetrical-channel pump. Further, motivated by these studies, Bazant *et al.* [3,4] significantly improved pumping velocity by using three-dimensional (3D) stepped electrodes for suppressing reverse flow. However, thus far, no attempts have been made for removing reverse flow by using asymmetrically stacked structures. In fact, the suppression of reverse flow occurs when ellipse metal posts are very near. In this paper, we focus on an ICEO pump that uses asymmetrical stacking as the origin for the suppression of the reverse flow, and we elucidate its design concept.

Figure 1 shows the schematic view of the hierarchically stacked asymmetrical ICEO pump considered in this study. As shown in Fig. 1, we place two second-generation ellipses with half lengths b to the left of a first-generation ellipse of length $2b$ in order to suppress the reverse flow of the first-generation ellipse. Similarly, we can suppress the reverse flow of the second-generation ellipse by placing two third-generation ellipses of lengths $b/2$ to the left of the second-generation ellipse. By repeating this procedure, we can obtain a hierarchically stacked asymmetrical structure. A pump that includes ellipses from first-generation ellipses to Nth-generation ellipses is termed an Nth-generation pump. In the above explanation, we consider a type-A stacking pump that suppresses the reverse flows of both sides of the first-generation ellipse; however, it is possible to consider other types of pumps (type B and type C, shown in Fig. 2) that suppress the reverse flow of one side of the first-generation ellipse by the wall of a channel, while the reverse flow of the other side is suppressed by the hierarchically stacked asymmetrical structure.

By considering the hierarchically stacked asymmetrical structure as the origin of the suppression of the reverse flow, we estimate the average flow velocity U_p of the pump as follows:

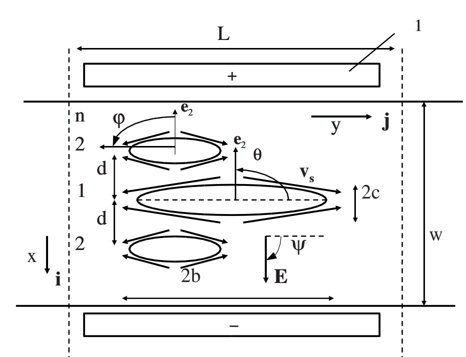

FIG. 1. Schematic view of hierarchically stacked asymmetrical ICEO pump. (1) Pair of electrodes. Here, $\psi=\theta=\pi/2$ rad, length $L=2.25w$, width $w=100$ μm, and $V_0=2.38$ V is applied to the electrodes. The ellipse has two semiaxes (b,c) with unit vectors $(\boldsymbol{e}_1,\boldsymbol{e}_2)$ that define the orientation of each semiaxis.

*sugioka.hideyuki@canon.co.jp

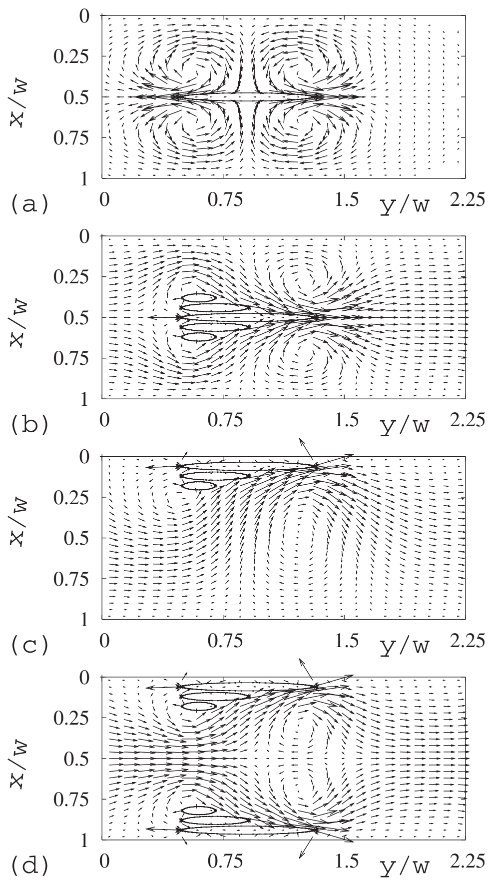

FIG. 2. Flow field of stacking pump without coatings. (a) Type-A pump ($N=1$, $U_p=0$ mm/s). (b) Type-A pump ($N=3$, $U_p=1.31$ mm/s). (c) Type-B pump ($N=3$, $U_p=0.97$ mm/s). (d) Type-C pump ($N=3$, $U_p=1.52$ mm/s). Here, $U_b=16$ mm/s, $E_0=23.8$ kV/m, $d/w=0.06$, $\delta/w=0.01$, and $c/w=0.025$, where $\delta=d-2c$. In the calculation, we used 50 to 72 elements for each ellipse.

$$U_p \approx \frac{4}{3}\left(1-\left(\frac{1}{4}\right)^{N-1}\right)\eta_{\rm n}\eta_k^{\sigma_k}\eta_{k_1}\eta_0 v_{\rm s}^{\rm max} - 0.4\,\eta_n v_{\rm s}^{\rm max}\frac{\delta}{w}, \tag{1}$$

where the first term ($U_p^{\rm forward}$) describes the forward pumping, the second term ($U_p^{\rm reverse}$) describes the reverse pumping that is a function of a gap δ ($=d-2c$), $v_{\rm s}^{\rm max}$ is the maximum slip velocity of an ellipse, η_0 is the intrinsic efficiency of a half-coating pump, η_k [$\approx(w-K)/w$] and η_{k_1} [$\approx(w-K_1)/w$] are the effect of narrowing of the channel, K and K_1 are the width of objects obstructing fluid flow [$K=2c(2N-1)+2\delta(N-1)$, $2cN+\delta(N-1)$, $4cN+2\delta(N-1)$, $K_1=2c$, $2c+\delta$, $4c+2\delta$, $\sigma_k=1.9$, 0.7, and 0.7 for type-A, -B, and -C pumps, respectively], and η_n is the effect of the number of the elliptical metal posts ($\eta_n=1$ for type-A and -C pumps; $\eta_n=0.5$ for type-B pump). It should be noted that

$$U_{p0} \approx \eta_{k_1}^{0.7}\eta_0 v_{\rm s}^{\rm max} \tag{2}$$

is the average flow velocity of the half-coating pump corresponding to the first-generation ellipse.

We consider a two-dimensional (2D) quasistatic Stokes flow without Brownian movement; that is, we consider the limit in which the Reynolds number Re tends to zero and the Peclet number is infinite. We assume the ellipse posts to be polarizable in an electrolytic solution under a dc or ac electric field. The motion of the surrounding fluid must satisfy the Stokes equations modified by the inclusion of an electrical stress. However, using a matched asymptotic expansion [8], we can reduce them to the classical Stokes equations as follows:

$$\mu\nabla^2\boldsymbol{v} - \boldsymbol{\nabla}p = 0, \quad \boldsymbol{\nabla}\cdot\boldsymbol{v} = 0, \tag{3}$$

$$\text{on metal } (\boldsymbol{E}\neq 0)\text{: } \boldsymbol{v} = \boldsymbol{v}_{\rm s}, \tag{4}$$

$$\boldsymbol{v}_{\rm s} = \frac{1}{2}U_b(\beta+1)^2 q_b^{-1}\sin 2(\psi+\varphi+\theta)\boldsymbol{t}, \tag{5}$$

where $q_b=\sqrt{\cos^2\varphi+\beta^2\sin^2\varphi}$, U_b ($=\epsilon b E_0^2/\mu$) is the representative velocity, $\beta=c/b$, $\boldsymbol{x}$ ($=-b\sin\varphi\boldsymbol{e}_1+c\cos\varphi\boldsymbol{e}_2$) is the surface position of metals parametrized by φ, $\boldsymbol{t}=-q_b^{-1}(\cos\varphi\boldsymbol{e}_1+\beta\sin\varphi\boldsymbol{e}_2)$ is the tangential unit vector of the surface position, electric field $\boldsymbol{E}=\cos\psi\boldsymbol{j}+\sin\psi\boldsymbol{i}$, $\boldsymbol{e}_2=\cos\theta\boldsymbol{j}-\sin\theta\boldsymbol{i}$, $\boldsymbol{e}_1=\sin\theta\boldsymbol{j}+\cos\theta\boldsymbol{i}$, where $\boldsymbol{i}$ and $\boldsymbol{j}$ are orthogonal unit vectors of the Cartesian coordinate system, μ ($\sim$1 mPa·s) is the viscosity, $\boldsymbol{v}$ is the velocity, $\boldsymbol{v}_s$ is the slip velocity, p is the pressure, ϵ ($\sim 80\epsilon_0$) is the dielectric permittivity of the solvent (typically water), and ϵ_0 is the vacuum permittivity. It should be noted that the maximum absolute value of $\boldsymbol{v}_s$ is

$$v_s^{\rm max} = U_b(\beta+1)^2\sin\varphi_0/\sqrt{1+\beta} \tag{6}$$

at $\varphi_0=\tan^{-1}\sqrt{1/\beta}$ when $\psi=\theta=\pi/2$. We calculate the flow fields of the ICEO pump by the boundary element method using Eqs. (3) and (4). In particular, to obtain a precise flow field near the wall and the metal surfaces, we use analytical integration to obtain the elements of the matrix of the boundary element method (50 to 72 elements for each ellipse). It is noteworthy that the Gauss integration produces a large error when ellipses are very near.

Figure 2 shows the flow field for the stacking pump when $b/w=0.4$, $c/w=0.025$, $U_b=16$ mm/s ($E_0=23.8$ kV/m), $d/w=0.06$, and $\delta/w=0.01$. On the one hand, for the first-generation pump shown in Fig. 2(a), we observe a symmetrical quadrupolar electro-osmotic flow around an ellipse post, and the net flow is zero because the forward flow of the left-hand part of the ellipse cancels the reverse flow of its right-hand part. On the other hand, the type-A, -B, and-C stacking pumps [whose flow fields are shown in Figs. 2(a)–2(c), respectively] function efficiently, i.e., the reverse flow is suppressed by the hierarchically stacked asymmetrical alignment of the ellipses, probably because the amount of the reverse pumping is limited in the level of $0.4v_s^{\rm max}\delta$. Further, the forward flow is stimulated by the increase of the surface of the forward slip velocity.

Figure 3 shows the performance of the asymmetrical stacking pump. As shown in Fig. 3(a), the suppression of the flow diminishes as the gap increases. Further, as predicted in Eq. (1), the reverse flow is considerably suppressed at the small gap ($\delta/w=0.01$). Here, U_p is almost a straight line at least for $\delta/w<0.1$ without depending on the value of c/w. The ultimate reason for having this behavior is that the re-

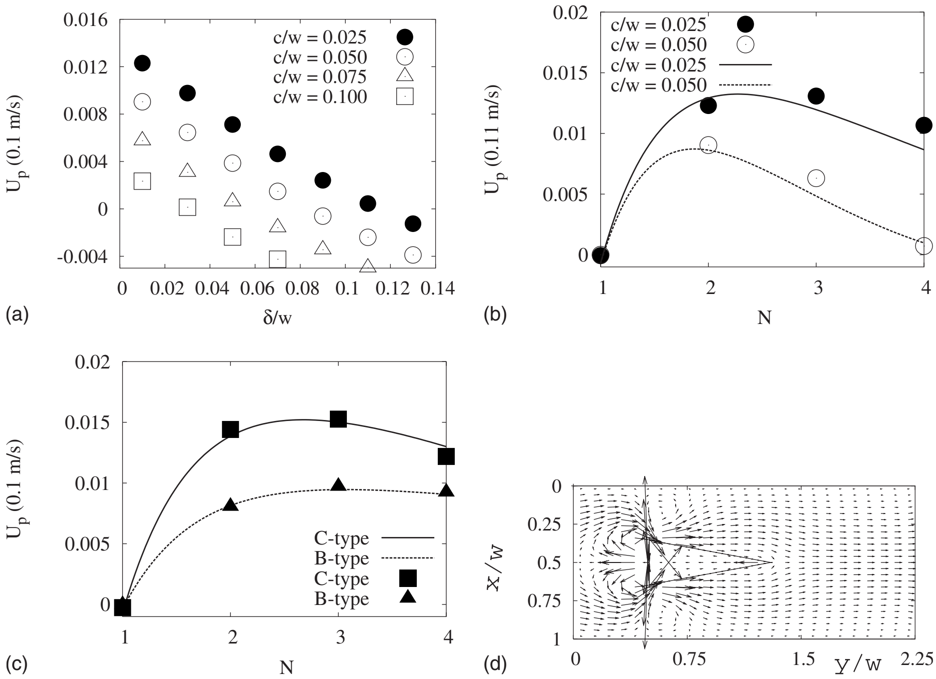

FIG. 3. Performance of asymmetrical stacking pump ($E_0 = 23.8$ kV/m, $\eta_0 = 0.12$). The lines show the analytical results obtained by Eq. (1). The symbols show the numerical results obtained by the boundary element method. (a) U_p vs δ for type-A pump at $N=2$. At $\delta/w=0.01$, the reverse flow is suppressed considerably. (b) U_p vs N for type-A pump. The maximum performance is 1.31 mm/s at $N=3$ when $c/w=0.025$ and $b/w=0.4$. (c) U_p vs N for type-B and type-C pumps. The maximum performances are 1.52 and 1.97 mm/s for type-C and type-B pumps, respectively, when $N=3$, $b/w=0.4$, and $c/w=0.025$. (d) Flow field of triangle metal post pump. Here, $w_h/w=0.29$, $L_b/w=0.8$, and $U_p = 0.11$ mm/s.

verse pumping is just proportional to δ/w because the amount of reverse flow is limited by the narrowest gap δ without depending on the curvature of elliptical posts. Further, a kind of adjustment mechanism works for the changes of the gradient $dU_p/d(\delta/w)$ when c/w changes as predicted in Eq. (1). That is, as c/w increases from 0.025 to 0.1, $dU_p^{\text{forward}}/d(\delta/w)$ changes from -6 to -3 mm/s, whereas $dU_p^{\text{reverse}}/d(\delta/w)$ increases from 7 to 8 mm/s. Thus, $|dU_p^{\text{inverse}}/d(\delta/w)|$ becomes approximately constant (~ 12 mm/s) without depending on the value of c/w. Here, we set $\eta_0=0.12$, and U_p is calculated on the boundary of the inlet ($y=0$ and $0<x<w$). Thus, we believe that the suppression of the reverse flow in the stacking pump occurs because a small gap limits the amount of the reverse pumping. Although the reverse flow is not completely suppressed for finite δ, a small gap that keeps unwanted slip velocities is intrinsically required to suppress the reverse flow. If there is no gap, the reverse flow in the x direction remains on the left-hand part of the pump, and it degrades the performance of the pump. Figures 3(b) and 3(c) show the dependence of the U_p values of the type-A, -B, and -C pumps on N. We compare the numerical results with theoretical results obtained using the simple model expressed in Eq. (1). Although these results are not in complete agreement with each other, both show that the effect of flow resistance is dominant. If we neglect the narrowing of the channel, U_p increases monotonously as N increases. However, in reality, U_p attains the maximum value at an optimum N in a real channel because flow resistance also increases. When $N=3$, $b/w=0.4$, and $c/w=0.025$, the maximum $U_p=1.31$, 0.97, and 1.52 mm/s for type-A, -B, and-C pumps, respectively. Note that a triangle metal post pump which shape and size are similar to a third-generation stacking pump changes the direction of reverse flow and shows the pumping performance ($U_p = 0.11$ mm/s) as shown in Fig. 3(d). However, the triangle metal pump cannot suppress the reverse flow considerably. Here, w_h $[=2c(2N-1)+2\delta(N-1)=0.29w]$ and L_h ($=2b=0.8w$) are the base length and the height of the triangle. Thus, the stacking pump is conceptually different from the irregular-shaped metal pump.

Figure 4 shows the performance of the half-coating pump. Figure 4(a) shows the flow of the optimum single half-coating pump at $c/w=0.15$ when $b/w=0.4$. Figure 4(b) shows the dependence of U_p on c. For this case, we compare the numerical results with the theoretical results obtained by the simple model expressed in Eq. (2). Here, $K_1=2c$. Although these results are not in complete agreement, both show that the effect of flow resistance is dominant. In a real channel, the pumping performance is the optimum at an optimum c because flow resistance also increases. As observed in Fig. 4(b), the maximum performances of the half-coating pump are $U_p=2.13$, 1.72, and 1.34 mm/s at $c/w=0.15$, 0.2, and 0.25 under the conditions $b/w=0.4$, 0.3, and 0.2, respectively, when we apply $V_0=2.38$ V to a channel with a width $w=100$ μm. Therefore, the performances of the type-C, -A, and -B stacking pumps are evaluated to be approximately 71, 61, and 46%, respectively, of the performance of the optimum half-coating pump. Figure 4(c) shows the flow of the optimum multiple half-coating pump when $N=2$, $c/w = 0.025$, and $b/w=0.4$. Figure 4(d) shows the dependence of U_p on the number N of multiple half-coating pumps under the condition $c/w=0.025$. Here, the distance between the ellipses is $w/(N+1)$. If we neglect the flow resistance, U_p increases as N increases. However, because of the flow resistance, U_p has the maximum value in a real channel; the maximum values of U_p are 2.44, 1.72, and 1.34 mm/s at $N = 2$, 2, and 3 when $b/w=0.4$, 0.3, and 0.2, respectively. Similarly, lateral arrangements also face a flow resistance problem because of the potentially large width of an ellipse.

The performance of hierarchically stacked asymmetrical pumps (46–71%) is good because they can be fabricated without coating. Further, from Eqs. (1) and (6) we can esti-

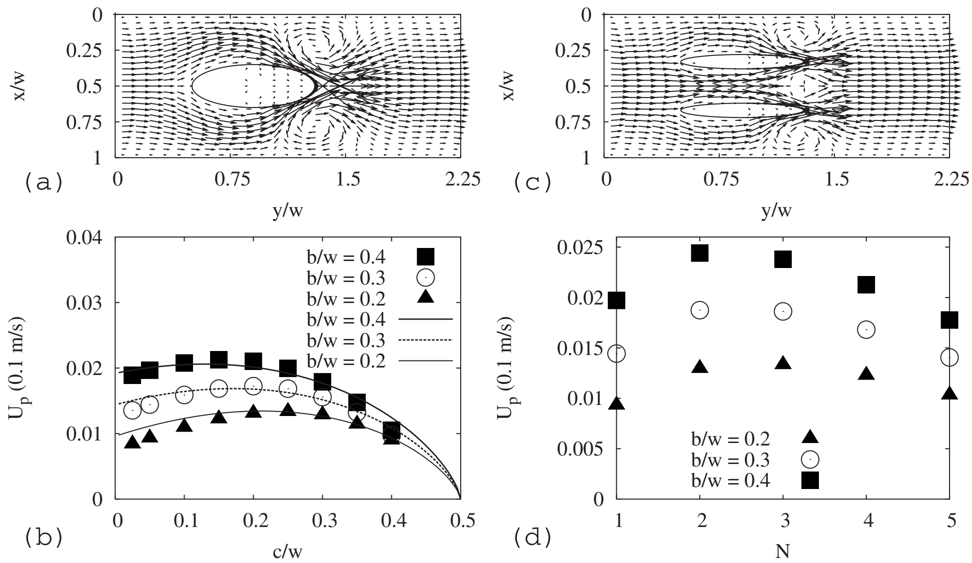

FIG. 4. Performance of half-coating pump (E_0=23.8 kV/m, η_0=0.12). (a) Flow of optimum single half-coating pump. Here, c/w =0.15, b/w=0.4, and U_b=16 m/s. (b) U_p vs c for the single half-coating pump. The U_p value is the maximum (2.13 mm/s) at c/w =0.15 when b/w=0.4. (c) Flow of optimum multiple half-coating pump. Here, N=2, b/w=0.4, and c/w=0.025. (d) U_p vs N for multiple half-coating pump. The U_p value is the maximum (2.44 mm/s) at N=2 when b/w=0.4 and c/w=0.025. The left-hand part of the ellipse was coated by insulators. The lines show the analytical results obtained by Eq. (2). The symbols show the numerical results obtained by the boundary element method.

mate $U_p \approx 1.33 U_b \eta_0$ for type-A and -C pumps in the limits $c \to 0$ and $N \to \infty$, whereas $U_{p0} \approx 2 U_b \eta_0 \eta_{k_1}^{0.7}$ for the half-coating pump at $c/b=1$. Because $\eta_{k_1}^{0.7} < 1$, the velocity of the stacking pump with a thin limit with infinite N is larger than 67% of that of the half-coating pump of the circular cylinder of the same length $2b$. Obviously, we can place such thin pumps in a channel with high density, large slip velocity, and small flow resistance. Further, such thin limit pumps with asymmetrically stacked metal posts can be used for planar structures, though an insulator may be required. Therefore, the stacking pump can dramatically improve the pumping performance in terms of flow rate, applied voltage, and applied electric field.

In conclusion, we have proposed ICEO pumps that employ asymmetrically stacked structures to suppress the reverse flow and examined the pumping performance by the boundary element method in conjunction with the double layer approximation and a simple model. The following are the conclusions of the numerical calculations. (1) The asymmetrical stacking configuration efficiently suppresses the reverse flow and yields ~mm/s velocity, which is 46–71% of the performance of an optimum half-coating pump. (2) The velocity of the stacking pump with a thin limit with infinite N is larger than 67% of that of the half-coating pump of the circular cylinder of the same length. The use of this stacking pump is expected to dramatically improve the pumping performance in terms of flow rate, applied voltage, and applied electric field. In the future, we intend to evaluate other stacking structures for suppressing reverse flow.

I am grateful to Professor E. Darve for the helpful discussions on the mathematical details of the calculation.

[1] M. Z. Bazant and T. M. Squires, Phys. Rev. Lett. **92**, 066101 (2004).
[2] T. Squires and M. Bazant, J. Fluid Mech. **509**, 217 (2004).
[3] J. Urbanski, T. Thorsen, J. Levitan, and M. Bazant, Appl. Phys. Lett. **89**, 143508 (2006).
[4] D. Burch and M. Z. Bazant, Phys. Rev. E **77**, 055303(R) (2008).
[5] A. Ramos, A. Gonzalez, A. Castellanos, N. G. Green, and H. Morgan, Phys. Rev. E **67**, 056302 (2003).
[6] A. Ajdari, Phys. Rev. E **61**, R45 (2000).
[7] L. H. Olesen, H. Bruus, and A. Ajdari, Phys. Rev. E **73**, 056313 (2006).
[8] M. Fair and J. Anderson, J. Colloid Interface Sci. **127**, 388 (1989).